

## **Cobalt immobilization by manganese oxidizing bacteria from Indian Ridge System**

Runa Antony<sup>1</sup>, Sujith P.P<sup>2</sup>, Sheryl O Fernandes<sup>2</sup>, Pankaj Verma<sup>3</sup>, Khedekar V.D<sup>2</sup>, Loka Bharathi P.A<sup>2\*</sup>

<sup>1</sup>Ice Core Laboratory, National Centre for Antarctic and Ocean Research, Headland Sada, Goa-403804

<sup>2</sup>Microbiology Laboratory, National Institute of Oceanography, Dona Paula, Goa-403 004

<sup>3</sup>National Centre for Cell Science, Pune

### **Abstract**

Co immobilization by two manganese oxidizing isolates from Carlsberg Ridge waters (CR35 and CR48) was compared with that of Mn at same molar concentrations. At a lower concentration of 10  $\mu\text{M}$ , CR35 and CR48 immobilized 22 and 23 fM Co cell<sup>-1</sup> respectively, which was 1.4 to 2 $\times$  higher than that of Mn oxidation, while at 10 mM the immobilization was 15 to 69 times lower than that of Mn. Scanning electron microscope and energy dispersive X-ray analyses of intact bacterial cells grown in 1 mM Co revealed Co peaks showing extracellular binding of the metal. However, it was evident from transmission electron microscope analyses that most of the sequestered Co was bound intracellularly along the cell membrane in both the isolates. Change in morphology was one of the strategies bacteria adopted to counter metal stress. The cells grew larger and thus maintained a lower than normal surface area-volume ratio on exposure to Co to reduce the number of binding sites. An unbalanced growth with increasing Co additions was observed in the isolates. Cells attained a length of 10-18  $\mu\text{m}$  at 10 mM Co which was 11-15 times the original cell length. Extensive cell rupture indicated that Co is harmful at this concentration. It is apparent that biological and optimal requirement of Mn is more than Co. Thus, these differences in the immobilization of the two metals could be driven by the differences in the requirement, cell physiology and the affinities of the isolates for the concentrations of the metals tested.

*Key words:* Bacteria, cobalt, immobilization, SEM-EDX, TEM, Carlsberg Ridge

## Introduction

Co is a biologically essential trace element that is required at low concentrations for metabolic activity. It is the central atom of Vitamin B<sub>12</sub> and is involved in diverse enzymatic reactions in microorganisms. It forms an important component of several proteins like aminopeptidase, prolidase, nitrile hydratase, glucose isomerase etc [23]. Co is an important micronutrient for marine phytoplankton and appears to be beneficial for growth at limiting Zn concentrations [30]. Low concentrations of Co and Zn have been shown to limit growth rates, affect cell size and chlorophyll concentrations in phytoplankton [35, 39, 41]. Thus, it is not surprising that phytoplankton have been implicated to dominate Co uptake in the oligotrophic surface waters of the Sargasso Sea and in the Peru upwelling region [29, 40].

The average concentration of Co in oceans is 0.3  $\mu\text{g L}^{-1}$  and in the Indian Ocean it is approximately 0.17–0.39  $\mu\text{g L}^{-1}$  [19]. Sources of Co in marine environments include metal containing industrial wastewaters and domestic discharge [3], radioactive <sup>60</sup>Co in nuclear wastes [38], chemical weathering and leaching of rocks [49], atmospheric inputs due to urban activity [16] and flyash released during burning of coal [6]. Yet another common abundant source is ferromanganese nodules spread at various sites over the ocean bed and at the sides of some seamounts [15]. Hydrothermal vent fluids release Co along with a broad spectrum of other metals like Mn, Al, Cu, Mo, Cd, Fe, Zn, Pb, Hg, As, Ga, and Tl [21, 28]. Some of these metals show a strong correlation in their concentration profiles. The striking similarity in the concentration profile of Co and Mn in the water column demonstrates that their biogeochemistries are closely coupled [4, 22, 26]. There are several lines of evidence that suggest a close relationship between Co and Mn oxidation. It is well recognized that bacteria catalyze the oxidation of Mn in marine environments [12, 17, 44, 45]. A number of studies have also implicated the role of bacteria in the oxidation of Co in marine environments. Due to the similarity in charge, size and oxidation potential of Co and Mn, it is quite possible that Mn oxidizing bacteria also oxidize Co. This is substantiated by the study of Moffett and Ho [29] and Lee and Tebo [25], implicating the role of Mn oxidizing bacteria in the oxidation of Co. In this study, an attempt has been made to demonstrate that the two Mn oxidizing isolates from Carlsberg Ridge (CR35 and CR48) could immobilize Co in the absence of Mn. The study also suggests that these Mn oxidizing bacteria could play a significant role in immobilizing and scavenging Co even in the absence of Mn.

## Materials and methods

### Growth and respiration studies

The effect of Co on growth and respiration of two Mn oxidizing bacterial isolates CR35 and CR48 [18] was monitored at Co amendments ranging from nanomolar to millimolar concentrations. Cells in the exponential growth phase were harvested from quarter strength nutrient agar plates (3.25 g nutrient broth and 15 g agar L<sup>-1</sup>) prepared in aged natural sea water and suspended in sterile saline (0.85%). The cell suspension was centrifuged at 2560×g for 10 min at 10°C (REMI Cooling Compufuge, R244 rotor). The supernatant was discarded and cell pellet was washed twice in physiological saline and thereafter re-suspended by vortexing (REMI Cyclomixer CM101). Filter sterilized 0.5% 2,3,5-Triphenyl tetrazolium chloride (TTC) (Hopkins and Williams Ltd., England.) was added to CoCl<sub>2</sub>.6H<sub>2</sub>O (Qualigens Galaxo India Ltd.) amended seawater tubes (pH 7.6-7.8) to obtain a final concentration of 0.025% TTC. The inoculum size was calculated by direct cell counts using a Neubauer counting chamber. The initial cell counts ranged from 5×10<sup>7</sup>-5.4×10<sup>7</sup> cells ml<sup>-1</sup>. The cells were observed under bright field at 600X magnification (BX61 Olympus microscope). Control tubes without metal were also maintained. The experiment was conducted in triplicates and the tubes were incubated in the dark at 22 ± 1°C for a period of 30 days. After the incubation period, the numbers of respiring and non-respiring cells were counted. Experiments were also run parallelly to determine the growth characteristics of the isolates under the influence of Co at 5-day intervals for a period of 30 days. Cells capable of catabolizing any substrate reduce TTC to deep red formazan and therefore appear red in color. The reduction of TTC is a result of electrons passing from the substrate (cobalt) through the enzymatic machinery of the cell and ultimately onto TTC. The amount of TTC reduced to formazan at the end of the incubation period was estimated by centrifuging the samples at 6550×g for 10 min at 10°C and suspending the cell pellet in 3 ml methanol (Qualigens Galaxo India Ltd.). After overnight extraction in methanol the tubes were again spun at 6550×g for 10 min at 10°C. The supernatant (200 µl) was analyzed spectrophotometrically at 520 nm (Thermo Multiskan Spectrum).

### Co immobilization

The Co immobilizing capacity of strains CR35 and CR48 was tested at Co concentrations of 10 µM, 100 µM, 1 mM and 10 mM. Uninoculated control tubes were maintained for each metal concentration to

measure the rate of auto oxidation. The samples were spun at  $2560\times g$  for 10 min at  $10^{\circ}\text{C}$ . Residual Co concentration in 1 ml of the supernatant was analyzed spectrophotometrically at 500 nm [8].

#### Scanning electron microscope (SEM) and Energy dispersive X-ray (EDX) analyses

A scanning electron microscope equipped with an energy dispersive X-ray spectrometer (SEM-EDX) was used to observe the morphology of the isolates incubated in the presence of Co. Thin smears of the culture from representative Co amended tubes were prepared on glass slides ( $1 \times 0.5''$ ). The slides were subjected through a series of increasing concentrations of acetone (Nice Chemicals Pvt. Ltd., India) from 10, 30, 50, 70, 90 and 100%. After air-drying, the dried slides were firmly fixed on metal stubs using a conductive adhesive and then coated with a film of Au using a gold sputter coater. The JEOL JSM-5800 Scanning Electron Microscope was used to observe cellular morphology. Bacterial cell dimensions were calculated directly from the SEM photographs. The cell volume and surface area were calculated as described by Chakravarty and Banerjee [7]. For EDX analysis, the bacterial isolates grown in seawater with and without added 1 mM  $\text{CoCl}_2.6\text{H}_2\text{O}$  were harvested and washed three times with sterile 0.85% saline and once with acetone by centrifugation at 8000 rpm for 15 min at  $4^{\circ}\text{C}$  and air-dried. The samples were powdered with a micro pestle in 2 ml eppendorf tubes. An EDX analysis was done on selected areas of intact cells at an accelerating voltage of 15 kV.

#### Transmission electron microscopy

Co is an electron-opaque metal and its uptake into the bacterial cell is likely to show up as an electron-dense region under an electron microscope. The bacterial isolates CR35 and CR48 were grown in 500 ml of 0.1% nutrient broth with and without 100 and 1000  $\mu\text{M}$  Co ( $\text{CoCl}_2.6\text{H}_2\text{O}$ ) for 48 hrs at  $25 \pm 1^{\circ}\text{C}$ . The cells were harvested by centrifuging at 8000 rpm for 5 min at  $4^{\circ}\text{C}$ . The cell pellets were washed twice in 0.85% saline and thereafter twice in 10 mM HEPES buffer (pH 8.0). The cells were then fixed with 2.5% glutaraldehyde (final concentration) in 1 ml of HEPES buffer and were used for transmission electron microscope (TEM) analysis. Sample processing for TEM was carried out following the procedures outlined by Hayat [20]. A FEI Morgagni 268D transmission electron microscope was used to observe Co immobilization by the bacterial cells.

## Analysis of 16S rRNA gene sequence

16S rRNA gene of both strains was isolated and their sequence determined at National Centre for Cell Science, Pune. The 16S rRNA gene sequence of CR35 (1515 bp) and CR48 (1291 bp) were compared with reference 16S rRNA gene sequences available in GenBank, EMBL and DDBJ using the BLAST program of the National Centre for Biotechnology Information (NCBI). Phylogenetic analysis was carried out using the BioEdit and Mega 4.1 software package.

## Results

### Effect of Co on growth and respiration

CR35 showed maximum tolerance at 100  $\mu\text{M}$  Co while CR48 tolerated a maximum of 10  $\mu\text{M}$  Co (Fig. 1a, b). At 100  $\mu\text{M}$  concentration, total count of CR35 increased by 1.7 times after 30 days of incubation at  $22 \pm 1^\circ\text{C}$ . At the concentration of 10  $\mu\text{M}$ , the cell counts of CR48 increased by 2 times after 30 days. A reduction in growth was observed in CR35 at concentrations above 100  $\mu\text{M}$  and in CR48 at concentrations above 10  $\mu\text{M}$ . The background increase in control without metal was negligible. At the end of the incubation period, the percentage of respiring cells of CR35 at 100  $\mu\text{M}$  Co and CR48 at 10  $\mu\text{M}$  Co accounted for only 46 and 47% of the total count. At the respective concentrations, respiration of CR35 (calculated only for respiring cells) was 1095 fg formazan cell<sup>-1</sup> and CR48 was 2350 fg formazan cell<sup>-1</sup>. However, maximum respiration in CR35 was noted at a much lower concentration of 10 nM (Fig. 1b). It was 3600 fg formazan cell<sup>-1</sup> which was nearly 3 times higher than that at 100  $\mu\text{M}$  Co. In contrast, CR48 showed the highest respiration of 11430 fg formazan cell<sup>-1</sup> at 100 nM Co (Fig. 1a). Since CR48 and CR35 showed the highest tolerance at 10  $\mu\text{M}$  and 100  $\mu\text{M}$  Co, respectively, the influence of the metal on the growth of these isolates was determined with time at the respective Co concentration. Co appeared to have a stimulatory effect on the growth of the isolates. Both total and respiring cell counts were higher when the isolates were grown in seawater amended with Co than in controls without Co. The respiring cell counts of CR48 increased rapidly from 0-day onwards (Fig 2a) while that of CR35 were observed only after day 10 (Fig 2b). Both CR48 and CR35 showed the highest increase in cell numbers on day-25 with counts increasing from  $1.84 \times 10^7$  to  $3.41 \times 10^7$  cells ml<sup>-1</sup> in CR48 and  $1.73 \times 10^7$  to  $2.15 \times 10^7$  in CR35.

## Cell morphology

Interestingly, SEM examination of the cultures revealed an increase in cell size and change in morphology of the original cells in increasing concentrations of Co at the end of 30 days growth (Table 1). SEM micrographs of CR48 grown at 10 nM Co addition revealed that the cells were oval shaped and 3-5 times larger than control cells ( $0.92\text{-}1.2 \times 0.6\text{-}0.7 \mu\text{m}$ ) ( Electron micrograph 3A and 3B), while they became elongated on exposure to 10  $\mu\text{M}$  (Electron micrograph 3C). Further addition (400  $\mu\text{M}$ ) produced long rods some of which showed a bulge at one end (Electron micrograph 3D). Higher concentration of 1 mM appeared to have a more pronounced effect on the cells as they increased in length by 5-6 times while a few cells were punctured (Electron micrograph 3E). The most dramatic effect however, was seen at 10 mM concentrations where the cells attained an unusually large size (10-18  $\mu\text{m}$ ) and were subsequently ruptured at the polar ends (Electron micrograph 3F). In most cases the damage left behind broken empty ghost cells.

The effect of Co on cellular morphology at different time intervals showed distinct morphological changes as evident from SEM micrographs. Cells existed as short rods ( $1\text{-}1.3 \times 0.53\text{-}0.62 \mu\text{m}$ ) in untreated cultures (Electron micrograph 4A). After two days, the cells increased in size to  $0.54\text{-}3.93 \times 0.61\text{-}3.9 \mu\text{m}$  and transformed to spherical forms, occurring in clusters or chains and less frequently as single cells (Electron micrograph 4B). Subsequent observations on day 4 and 6 also showed the presence of clusters and chains of spherical cells. However, after 8, 10 and 15-day exposure, lenticular cells were observed along with the spherical forms (Electron micrograph 4C). The size of the lenticular cells was  $0.72\text{-}4.17 \times 0.65\text{-}2.97 \mu\text{m}$ . The lenticular cells formed about 4, 9 and 25% of the total cells on day 8, 10 and 15, respectively. But on day 15, about 10% of the lenticular cells began to develop a depression along the central axis of the cell. By day 20, about 87% of the cells transformed into unusually long rods measuring  $1.5\text{-}21.1 \times 0.44\text{-}0.67 \mu\text{m}$  in size (Electron micrograph 4D). By day 25, most of the remaining lenticular forms developed a pronounced depression in the centre of the cell giving a 'doughnut-like' appearance (Electron micrograph 4E) and some cells appeared fused with each other. After 30-day exposure to Co, abnormally large cells of average size  $6.3 \times 3.26 \mu\text{m}$  were observed (Electron micrograph 4F). About 34% of these cells were found to be punctured. Determination of surface area to volume ratio of the bacterial cells revealed that the ratio decreased when exposed to Co. The most significant decrease occurred after 2 day exposure when the surface area to volume ratio decreased from 8.7 to 3.1. After 30-day exposure, the ratio further dropped to 1.54.

## Co immobilization

CR35 showed maximum immobilization of 13.8  $\mu\text{M}$  Co (130.8 fM Co cell<sup>-1</sup>) at 1mM Co amendment at the end of 30 days. At 10 mM Co amendment the amount of Co immobilized dropped to 6  $\mu\text{M}$  with 81.9 fM Co immobilized cell<sup>-1</sup> (Fig. 5b). CR48 also showed a similar trend and the uptake peaked at 1 mM Co concentration with an immobilization of 138  $\mu\text{M}$  Co (2361 fM Co cell<sup>-1</sup>) at the end of the incubation (Fig. 5a).

CR48 not only showed better growth and respiration than CR35 at concentrations of 1  $\mu\text{M}$  to 10 mM, it was also able to immobilize Co better at these concentrations. At 10  $\mu\text{M}$  Co amendment, CR48 immobilized 2  $\mu\text{M}$  Co (24.9 fM Co cell<sup>-1</sup>) which was almost the same as that of CR35. But at all other concentrations tested, Co immobilization by CR48 was about 3 - 18 times higher than that of CR35.

## SEM-EDX analyses

The EDX spectra showed detectable peaks of Co on individual cells of CR35 and CR48 grown in the presence of Co (Figs 6B, 6D), while control cells lacked any detectable Co (Figs 6A, 6C). Although Co was present on the external cell surface of both isolates its concentration was very low in CR48. The EDX pattern of selected areas on individual cells of CR35 displayed Co peaks showing 2.45% Co while CR48 had peaks showing about 0.71% Co (Table 2).

## TEM analyses

TEM observations of thin cross sections of the bacterial cells exposed to Co allowed the detection of electron dense areas within the cell especially at the cell membrane indicating intracellular accumulation of Co. An exopolymeric layer was usually seen surrounding the cells of CR35 which was less frequently seen in CR48. TEM micrograph 7B showed Co accumulation in CR35 grown in 1 mM Co amended seawater. CR35 was found to immobilize Co intracellularly as well as in the exopolymeric matrix. However, TEM micrographs of CR48 showed intracellular accumulation of Co more frequently and extracellular accumulation very rarely (TEM micrograph 7D).

## Phylogenetic analysis

Sequencing of the 16S rRNA gene indicated that both strains belonged to the genus *Halomonas* showing 99% similarity to *Halomonas cupida*. The genus *Halomonas* forms a group within the  $\gamma$ -Proteobacteria.

The 16S rRNA gene sequences of the isolates have been deposited in the GenBank database. The accession numbers of the sequences are as follows: EU088257 for CR35 and EU088258 for CR48.

## **Discussion**

The study shows the tolerance of CR35 and CR48 to high concentrations of Co. The highest tolerance was seen at 10  $\mu\text{M}$  in CR48 and 100  $\mu\text{M}$  concentration in CR35. At higher concentrations (>10 and 100  $\mu\text{M}$ ) cell counts gradually declined, indicating stress to the organism. Though Co has important biological functions, it is required only at low concentrations and can become toxic at micro and millimolar concentrations [14, 32]. Metals become toxic to the organism when their concentration is higher than the demand for metabolism, resulting in inhibition of metabolic pathways usually by strongly binding to enzymes, forming unwanted radicals or less stable reaction products [36]. The toxicity of Co appears to be due to unregulated cell growth triggered by internal sequestration of the metal, resulting in enlarged cells and their subsequent rupture. The control cells had normal morphology while cells grown in the presence of Co showed pronounced morphological irregularities with increasing concentrations of the metal. At concentrations above 100  $\mu\text{M}$  Co, the cells showed a protrusion at one end as though the cell contents are pressed against the cell wall. This may be due to weakening of the cell wall and its failure to resist the internal pressure. This may explain the subsequent rupture of the cell wall at high Co concentrations. The major role of the cell wall is to prevent the bursting of the cell caused by the internal pressure. Without the cell wall, the cell would undergo lysis [48]. Cobet et al [9] have observed similar morphological changes in *Arthrobacter marinus* sp. with increasing concentrations of nickel. They attributed these changes to continuation of cellular growth with cessation of cell division resulting in enlarged cells. Platinum-induced filamentous growth and inhibition of cell division in *E. coli* have been reported by Rosenberg et al [37]. Cells exposed to 1 mM Co showed various morphological changes on prolonged exposure to Co. Cells reacted to the presence of Co by reducing the cell surface to volume ratio. This reduction could represent an adaptive mechanism to counteract the toxicity of Co. Decrease in cell surface area would decrease metal binding sites at the cell surface. This adaptation would enable these isolates to tolerate higher concentrations of Co for longer duration. A similar response of cells on exposure to heavy metals has been reported by Chakravarty and Banerjee [7]. They have described the higher than normal cell volume of cells with respect to the cell surface as an adaptive strategy to counter heavy metal toxicity.



The present study also indicates the Co immobilizing potential of these Mn oxidizing isolates. Both isolates were found to immobilize Co intracellularly. But, CR35 was also found to immobilize Co extracellularly on the cell surface and in the exopolymeric matrix. TEM examination revealed intracellular sequestration of Co along the cell membrane. Intracellular accumulation of Co as inclusion bodies has been reported in some bacteria [2, 47]. The metal binding capacity of bacterial exopolymers is well known and has been extensively studied [27, 34]. The sequestration of metal by the exopolymeric matrix surrounding the bacterial cell reduces the direct toxic effect of the metal. This may explain why CR35 showed maximum tolerance at higher concentration (100  $\mu\text{M}$  Co) than CR48. Such adaptation has also been encountered in *Pseudomonas* [1]. Although SEM-EDX analysis showed deposition of Co on the external cell surface, TEM showed that more of the metal was also sequestered inside the cell.

Both strains could immobilize Co over a range of concentrations from 10  $\mu\text{M}$  to 10 mM. Lee and Tebo [25] have reported Co oxidation by a marine Mn oxidizing *Bacillus* at Co concentrations varying from trace levels to 100 mM. Krishnan et al [24] have reported Co immobilization at 10 mM concentration by bacteria isolated from Afanasiy Nikitin seamounts. The average immobilization rates of those isolates were 62 times higher than that of CR35 (0.22  $\mu\text{M day}^{-1}$ ) and 373 times higher than that of CR48 (1.33  $\mu\text{M day}^{-1}$ ). The high immobilization rates of these isolates may be attributed to the adaptability of the bacteria to the naturally high concentration of Co (1.23%) in the Co crusts from Afanasiy Nikitin seamounts [13]. Although no data is available on the concentration of Co in Carlsberg Ridge waters, ferromanganese nodules collected from Carlsberg Ridge were found to contain 0.07-0.21% Co [5]. The bacteria from Carlsberg Ridge waters are therefore accustomed to a much lower concentration of Co, which may explain their lower immobilization rates. Surprisingly, these isolates could immobilize Co at 10 mM, ie. at concentrations much higher than the ambient. However, the immobilization potential of CR48 at 10 mM was only 27% of the maximum Co immobilized at 1 mM (2361 fM Co cell<sup>-1</sup>). On the other hand, the immobilization at 10 mM Co by CR35 was about 63% of the maximum of 130.8 fM Co cell<sup>-1</sup> at 1 mM Co. The reduction in Co immobilization at higher metal concentration may be a strategy adopted by the bacteria to counteract metal toxicity. Diminished net accumulation of the metal ions based on an active efflux of metal ions has been described as a mechanism of metal resistance developed in prokaryotes [32]. Though both the isolates showed 99% similarity to the type strain *Halomonas cupida*, their response to the metals at various concentrations differed. This difference could be attributed to fine alterations in their gene expression.

A comparison of Co and Mn immobilization showed that the strains exhibited a different response to Co and Mn. In CR48, at lower concentrations of 10  $\mu\text{M}$  and 100  $\mu\text{M}$ , Co immobilized was 23  $\text{fM cell}^{-1}$  and 196.5  $\text{fM cell}^{-1}$ , respectively and is 1.4-3 times higher than that of Mn. But as concentration of metal increased, Co immobilization was found to be lower than that of Mn. At 10 mM concentrations, metal immobilization was 637.8  $\text{fM cell}^{-1}$  which is 15 times lower than that of Mn. CR35 also showed a similar trend. Although the trend in metal immobilization was the same in the two isolates, CR48 was able to immobilize both Co and Mn at a much higher rate than CR35. Though both Co and Mn form important components of metalloenzymes and proteins [10, 23, 33], Mn has several additional biological functions. The benefits of Mn oxidation by bacteria include protection from toxic heavy metals, predation, viruses and storage of an electron acceptor for later use in anaerobic respiration [46]. Sunda and Kieber [42] have demonstrated that Mn oxides can break down refractory organic matter into low molecular weight substrates that can be utilized by bacteria. Accumulation of Mn in *Deinococcus radiodurans* has been shown to provide resistance to  $\gamma$ -radiation [11]. Moreover in nature, where the concentration of Mn is several orders of magnitude higher than Co, it is quite likely that bacteria oxidize Mn at a higher rate than Co. Moffett and Ho [29] showed that specific rates for Mn oxidation in the Waquoit bay was 7-10 $\times$  faster than that of Co.

In the environment, where Mn concentrations are high, these strains could actively contribute to Mn oxidation. Since these bacteria are capable of immobilizing both elements, it is possible that these isolates could participate in the immobilization of these elements in specialized ecosystems like nodule, ridge and crust. Bacterially mediated incorporation of Co in nodules can occur through either direct or indirect processes. Indirect catalysis could occur by initial adsorption and the subsequent oxidation of Co(II) to Co(III) on the surface of bacterially formed Mn oxide [31]. Tani et al [43] showed that biogenic Mn oxides have a high affinity for Co(II) and this binding is highly irreversible. This could have a marked impact on the concentration profile of Co in ridge ecosystems rich in manganese oxides and ferromanganese encrustations. It may also be possible that these bacteria directly catalyze the oxidation of Co. Sequence analysis of manganese oxidizing *Bacillus* sp., strain SG-1 by Lee and Tebo [25] revealed the presence of two genes that code for proteins involved in both Mn and Co oxidation, indicating that they may be oxidized via a common cellular mechanism. The ability of the isolates CR35 and CR48 to immobilize both these metals demonstrates that they could play a significant role in controlling the chemistry and distribution of Co and Mn in metal enriched marine environments such as ridge and hydrothermal vent systems. The metal immobilizing property of these autochthonous strains at

high metal concentrations suggests that these can be used as reliable tools in the bioremediation of metal contaminated waters.

## **Conclusion**

The adaptability of CR35 and CR48 to high metal concentrations and ability to immobilize Co and Mn suggest that these bacteria may also be capable of scavenging other metals in Carlsberg Ridge waters. Ecologically, the physiology of CR35 is more competitive than CR48 as it has dual strategies for countering metal toxicity. Nevertheless, these microbes could participate in the regulation of oceanic metal cycles and determine the fate of trace metals in marine environments.

## **Acknowledgement**

The authors thank the Directors; NIO, NCAOR and NCCS for support. Special thanks are due to Dr. Rahul Mohan of NCAOR for providing SEM facility. We acknowledge the services of AIIMS, Delhi for TEM analysis. We thank Dr. CT Achuthankutty, Visiting Scientist, NCAOR, for critical evaluation of the manuscript. This work was carried out under the project ‘Tectonic and Oceanic Processes along the Indian Ridge system and Back-Arc Basins’ funded by CSIR/DOD and led by Dr. KA Kamesh Raju. SPP acknowledges the Council of Scientific and Industrial Research, New Delhi, India, for the award of ‘Senior Research Fellowship’. The manuscript improved considerably by the critical evaluation of an anonymous reviewer. This is NIO contribution No xxxxxx.

## **References**

1. Appanna VD (1988) Stimulation of exopolysaccharide production in *Rhizobium meliloti* JJ-1 by manganese. *Biotechnol Lett* 10:205-206
2. Ariskina EV, Vatsurina AV, Suzina NE, Gavrish E Yu. (2004) Cobalt- and chromium-containing inclusions in bacterial cells. *Microbiologia* 73:199-203
3. Atlas L, Büyükgüngör H (2007) Heavy metal pollution in the Black Sea shore and offshore of Turkey. *Environ Geol* 52:469-476
4. Balistrieri LS, Murray JW, Paul B (1992) The biogeochemical cycling of trace metals in the water column of lake Sammamish, Washington: Response to seasonally anoxic conditions. *Limnol Oceanogr* 37:529-548

5. Banerjee R, Ray D (2003) Metallogenesis along the Indian Ocean Ridge System. *Curr Sci* 85:321-327
6. Benjamin, MM, Honeyman BD (1992) Trace metals. In: Butcher SS, Charlson RJ, Orians GH, Wolfe GV (eds) *Global Biogeochemical Cycles*, Academic Press Limited, pp 317-350
7. Chakravarty R, Banerjee PC (2008) Morphological changes in an acidophilic bacterium induced by heavy metals. *Extremophiles* 12:279-284
8. Chester R, Hughes MJ (1968) Scheme for the spectrophotometric determination of Cu, Pb, Ni, V and Co in marine sediments: Applied earth Science. *Trans Inst Min and Metallurgy* 77:37-41
9. Cobet AB, Jun. Wirsen C, Jones GE (1970) The effect of nickel on a marine bacterium, *Arthrobacter marinus* sp. nov. *J Gen Microbiol* 62:159-169
10. Culotta VC, Yang M, Hall MD (2005) Manganese transport and trafficking: Lessons learned from *Saccharomyces cerevisiae*. *Eukaryot Cell* 4:1159-1165
11. Daly MJ, Gaidamakova EK, Matrosova VY, Vasilenko A, Zhai M, Venkateswaran A, Hess M, Omelchenko MV, Kostandarithes HM., Makarova KS, Wackett LP, Fredrickson JK, Ghosal D (2004) Accumulation of Mn(II) in *Deinococcus radiodurans* facilitates gamma-radiation resistance. *Science* 306:1025-1028
12. Diem D, Stumm W (1984) Is dissolved Mn<sup>2+</sup> being oxidized by O<sub>2</sub> in absence of Mn-bacteria or surface catalysts? *Geochim Cosmochim Acta* 48:1571-1573
13. Dutta RK, Acharya RN, Chakravorty V, Nair AGC, Reddy AVR, Chintalapudi SN, Manohar SB (1998) Instrumental neutron activation analysis of ferromanganese oxide encrustations of Indian Ocean by the K<sub>0</sub> NAA method. *J Radioanal Nucl Chem* 237:91-96
14. Ehrlich HL (1997) Microbes and metals. *Appl Microbiol Biotechnol* 48:687-692
15. Ehrlich HL (2000) Ocean manganese nodules: Biogenesis and bioleaching possibilities. *Miner Metall Process* 17:121-128
16. Eisenreich SJ (1980) Atmospheric inputs of trace metals to Lake Michigan. *Water Air Soil Pollut* 13:287-301
17. Emerson S, Kalthorn S, Jacobs L, Tebo BM., Neilson KH., Rosson RA (1982) Environmental oxidation rate of manganese(II): bacterial catalysis. *Geochim Cosmochim Acta* 46:1073-1079
18. Fernandes SO, Krishnan KP, Khedekar VD, Loka Bharathi PA (2005) Manganese oxidation by bacterial isolates from the Indian Ridge System. *Biometals* 18:483-492
19. Hamilton EI (1994) The geobiochemistry of cobalt. *Sci Tot Environ* 150:7-39

20. Hayat MA (1972) Basic Electron Microscopy Techniques. New York, Van Nostrand Reinold
21. Kádár E, Costa V, Martins I, Santos RS, Powell JJ (2005) Enrichment of trace metals (Al, Mn, Co, Cu, Mo, Cd, Fe, Zn, Pb and Hg) of macro-invertebrate habitats at hydrothermal vents along the Mid-Atlantic Ridge. *Hydrobiologia* 548:191-205
22. Knauer GA, Martin JH, Gordon RM (1982) Cobalt in north-east Pacific waters. *Nature* 297:49-51
23. Kobayashi M, Shimizu S (1999) Cobalt proteins. *Eur J Biochem* 261:1-9
24. Krishnan KP, Fernandes CEG, Fernandes SO, Loka Bharathi PA (2006) Tolerance and immobilization of cobalt by some bacteria from ferromanganese crusts of the Afanasiy Nikitin Seamounts. *Geomicrobiol J* 23:31-36
25. Lee Y, Tebo BM (1994) Cobalt(II) oxidation by the marine manganese(II)-oxidizing *Bacillus* sp. strain SG-1. *Appl Environ Microbiol* 60:2949-2957
26. Lienemann CP, Taillefert M, Perret D, Gaillard JF (1997) Association of cobalt and manganese in aquatic systems: Chemical and microscopic evidence. *Geochim Cosmochim Acta* 61:1437-1446
27. Loaëc M, Olier R, Guezennec J (1997) Uptake of lead, cadmium and zinc by a novel bacterial exopolysaccharide. *Wat Res* 31:1171-1179
28. Metz S, Trefry JH (2000) Chemical and mineralogical influences on concentrations of trace metals in hydrothermal fluids. *Geochim Cosmochim Acta* 64:2267-2279
29. Moffett JW, Ho J (1996) Oxidation of cobalt and manganese in seawater via a common microbially catalyzed pathway. *Geochim Cosmochim Acta* 60:3415-3424
30. Morel FMM, Reinfelder JR, Roberts SB, Chamberlain CP, Lee JG, Yee D (1994) Zinc and carbon co-limitation of marine phytoplankton. *Nature* 369:740-742
31. Murray JW, Dillard JG (1979) The oxidation of cobalt(II) adsorbed on manganese dioxide. *Geochim Cosmochim Acta* 43:781-787
32. Nies DH (1992) Resistance to cadmium, cobalt, zinc, and nickel in microbes. *Plasmid* 27:17-28
33. Nies DH (1999) Microbial heavy-metal resistance. *Appl Microbiol Biotechnol* 51:730-750
34. Pal A, Paul AK (2008) Microbial extracellular polymeric substances: Central elements in heavy metal bioremediation. *Indian J Microbiol* 48:49-64
35. Price NM, Morel FMM (1990) Cadmium and cobalt substitution for zinc in a marine diatom. *Nature* 344:658-660

36. Raab A, Feldmann J (2003) Microbial transformation of metals and metalloids. *Sci Prog* 86:179-202
37. Rosenberg B, Renshaw E, Vancamp L, Hartwick J, Drobnik J (1967) Platinum-induced filamentous growth in *Escherichia coli*. *J Bacteriol* 93:716-721
38. Ryan MT, Lee MP, Larson HJ (2007) History and framework of commercial low-level radioactive waste management in the United States. Washington, DC, Advisory Committee on Nuclear Waste U.S. Nuclear Regulatory Commission
39. Saito MA, Moffett JW, Chisholm SW, Waterbury JB (2002) Cobalt limitation and uptake in *Prochlorococcus*. *Limnol Oceanogr* 47:1629-1636
40. Saito MA, Moffett JW (2004) Cobalt and nickel in the Peru upwelling region: A major flux of labile cobalt utilized as a micronutrient. *Global Biogeochem Cy* 18:GB4030
41. Sunda WG, Huntsman SA (1995) Cobalt and zinc interreplacement in marine phytoplankton: Biological and geochemical implications. *Limnol Oceanogr* 40:1404-1417
42. Sunda WG, Kieber DJ (1994) Oxidation of humic substances by manganese oxides yields low-molecular-weight organic substrates. *Nature* 367:62-64
43. Tani Y, Ohashi M, Miyata N, Seyama H, Iwahori K, and Soma M (2004) Sorption of Co(II), Ni(II), and Zn(II) on Biogenic Manganese Oxides Produced by a Mn-oxidizing fungus, strain KR21-2. *J Environ Sci Health Part A*, 39:2641-2660
44. Tebo BM (1991) Manganese(II) oxidation in the suboxic zone of the Black Sea. *Deep-Sea Res Suppl* 2, 38:883-905
45. Tebo BM, Bargar JR, Clement BG, Dick GJ, Murray KJ, Parker D, Verity R, Webb SM (2004) Biogenic manganese oxides: Properties and mechanisms of formation. *Annu Rev Earth Planet Sci* 32:287-328
46. Tebo BM, Johnson HA, McCarthy J K, Templeton AS (2005) Geomicrobiology of Mn(II) oxidation. *Trends Microbiol* 13:421-428
47. Vainshtein M, Suzina N, Kudryashova E, Ariskina E (2002) New magnet-sensitive structures in bacterial and archaeal cells. *Biology of the Cell* 94:29-35
48. Weibull C (1953) The Isolation of protoplasts from *Bacillus megatarium* by controlled treatment with lysozyme. *J Bacteriol* 66:688-695
49. Young RS (1957) The geochemistry of Cobalt. *Geochim Cosmochim Acta* 13:28-41

Table 1. Increase in cell size of isolate CR48 in response to a range of cobalt concentrations.

Sample	Average cell size ( $\mu\text{m}$ )	Cell elongation
Control	0.92 - 1.2 $\times$ 0.6 - 0.7	-
10 nM Co	2.9 - 6.1 $\times$ 1.8 - 3.3	3-5 $\times$
100 $\mu\text{M}$ Co	4.2 - 6.1 $\times$ 0.98 - 1.2	5 $\times$
1 mM Co	4.3 - 7.4 $\times$ 1 - 3.3	5-6 $\times$
10 mM Co	10 - 18 $\times$ 2.6 - 5.3	11-15 $\times$

Table 2. Elemental composition of the isolates obtained from EDX spectral analysis.

Element	Weight (%)	
	CR35	CR48
O	31.2	31.3
Na	11.0	16.89
Mg	5.03	0.70
Al	0.17	nd
Cl	3.72	22.28
K	0.41	nd
Ca	9.46	nd
Co	2.45	0.71
P	26.6	28.13
Total	100	100

nd- not detected

## Figure legends

- Fig. 1 Effect of increasing concentrations of Co on growth and respiration of CR48 (a) and CR35 (b). The graph depicts total and respiring cell counts observed at the end of the 30-day incubation period. Bars represent  $\pm$  standard deviation of mean (n=3).
- Fig. 2 Growth of CR48 in 10  $\mu$ M (a) and CR35 in 100  $\mu$ M (b) Co amended and unamended seawater. Graph depicts total and respiring cells.
- Fig. 3 Scanning electron micrographs of CR48 cultured without Co (A) and with the addition of 10 nM (B), 10  $\mu$ M (C), 400  $\mu$ M (D), 1 mM (E) and 10 mM (F).
- Fig. 4 Scanning electron micrographs of CR48 grown in the presence of 1 mM Co at different time intervals. Electron micrographs show cells on 0-day (A), 2-day (B), 15-day (C), 20-day (D), 25-day (E) and 30-day (F).
- Fig. 5 Co immobilization by CR48 (a) and CR35 (b). Bars represent  $\pm$  standard deviation (n=3).
- Fig. 6 EDX spectrum of CR48 grown in the absence (A) and in the presence of 1 mM Co (B) and of CR35 in the absence (C) and presence of 1 mM Co (D).
- Fig. 7 Transmission electron micrographs of thin sections of CR35 grown on unamended (A), 1 mM Co amended seawater (B) and of CR48 in unamended (C) and 1 mM Co amended seawater (D). Thin black arrows indicate intracellular metal accumulation and thick black indicates deposition in the exopolymeric matrix.



Fig 1

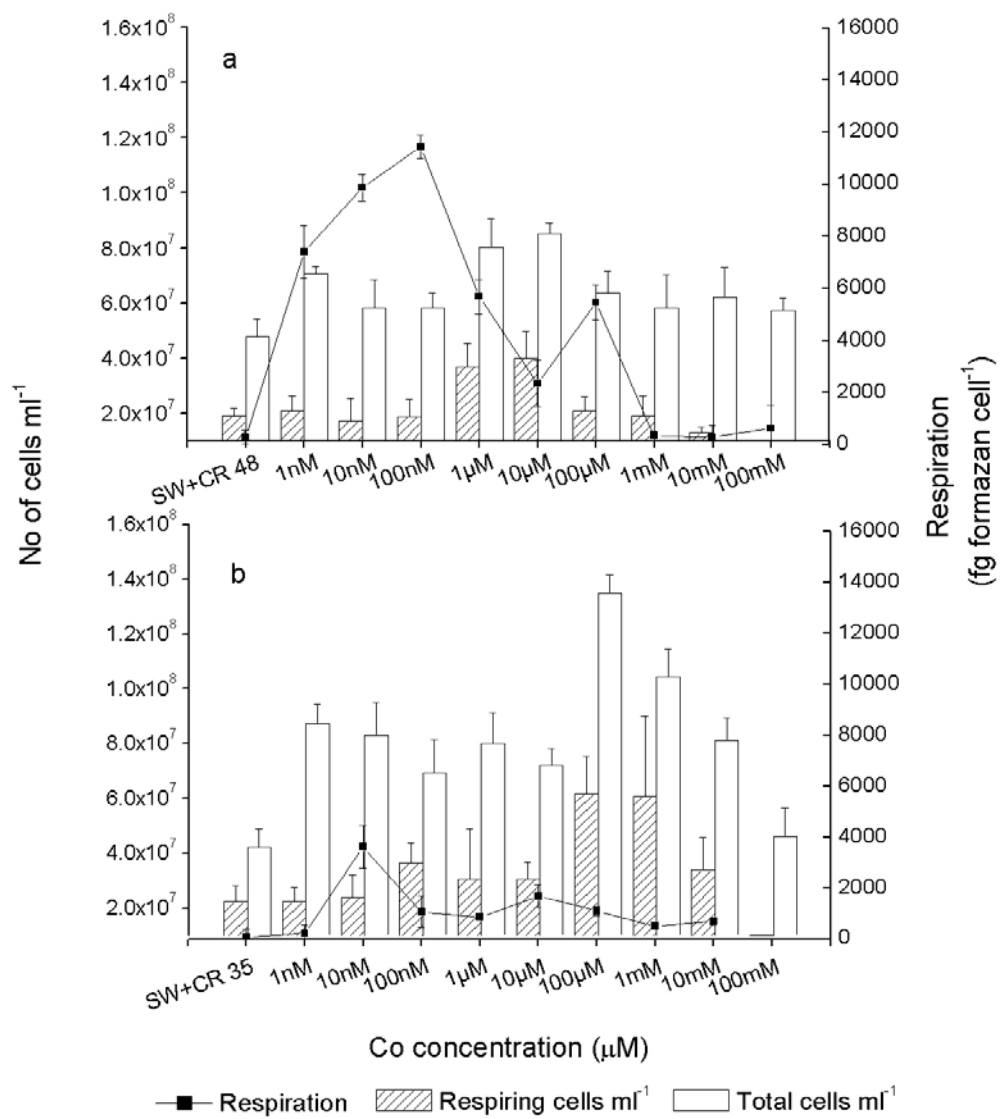


Fig 2

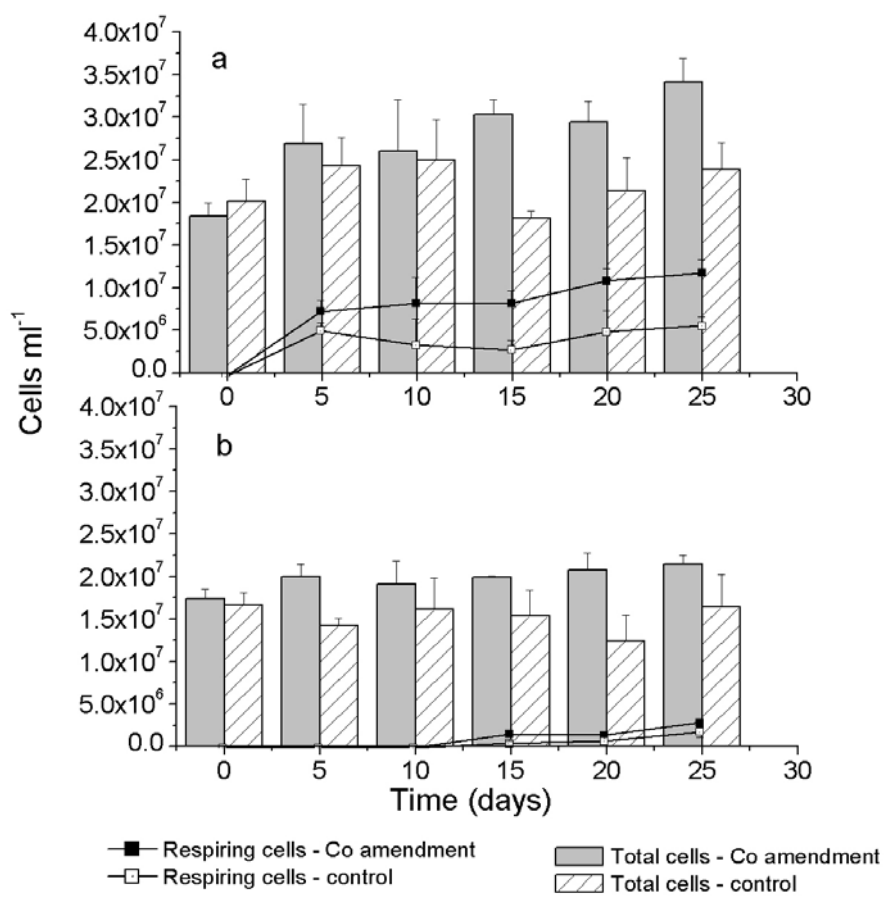


Fig 3.

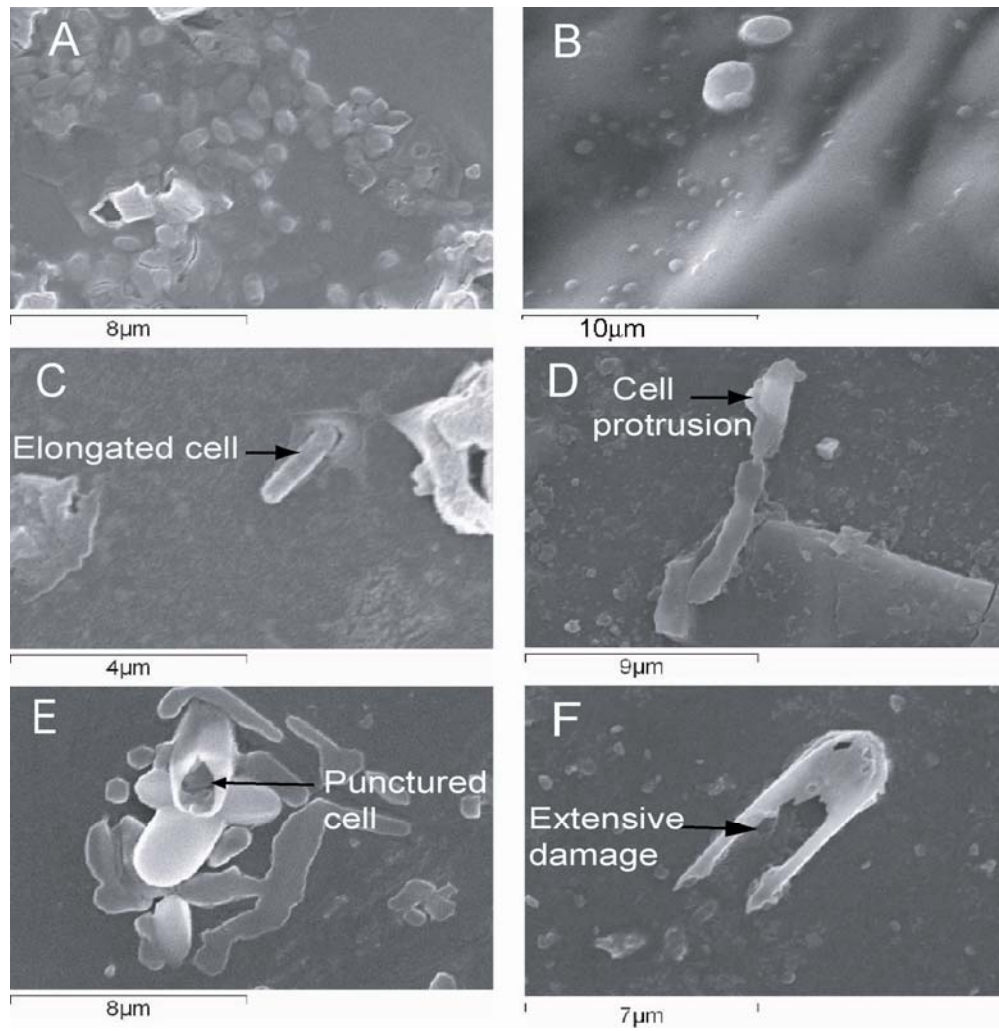


Fig 4.

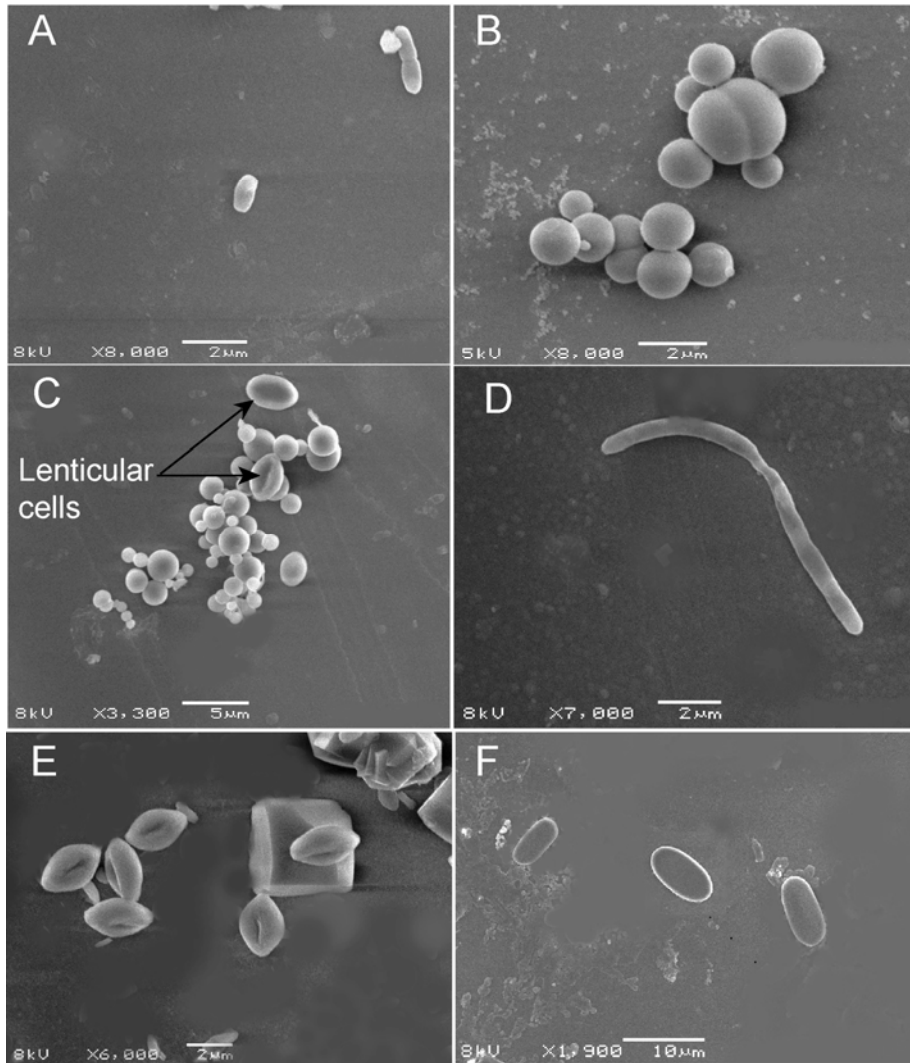


Fig 5.

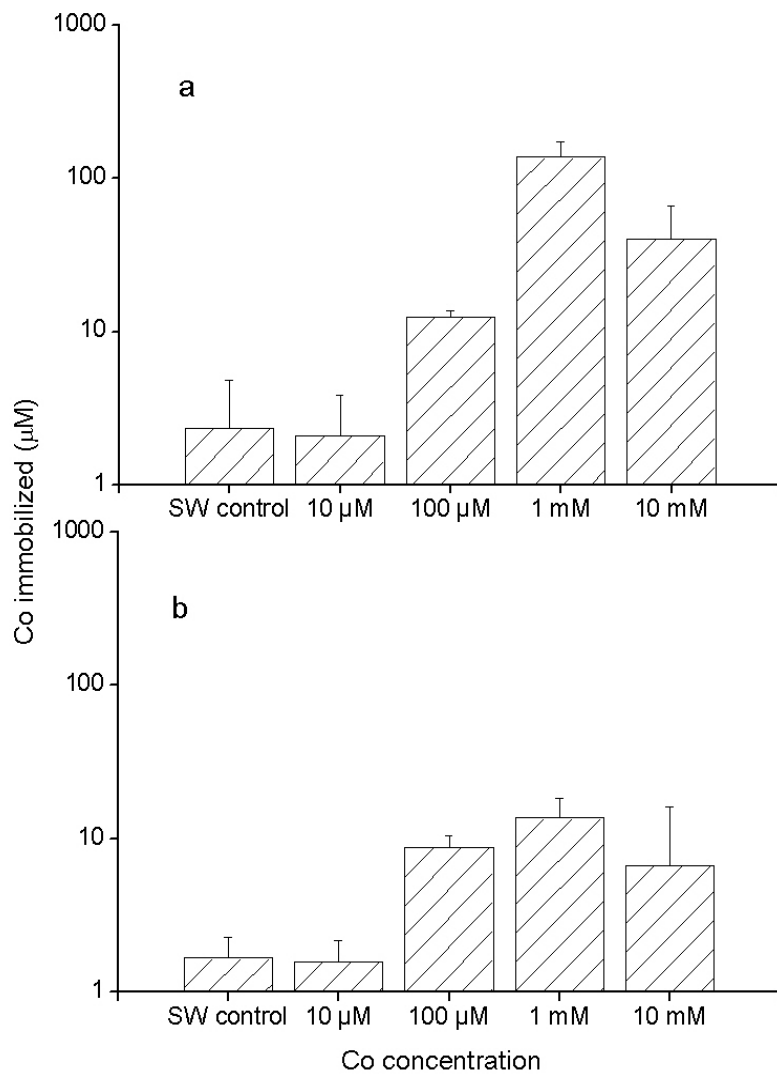


Fig 6.

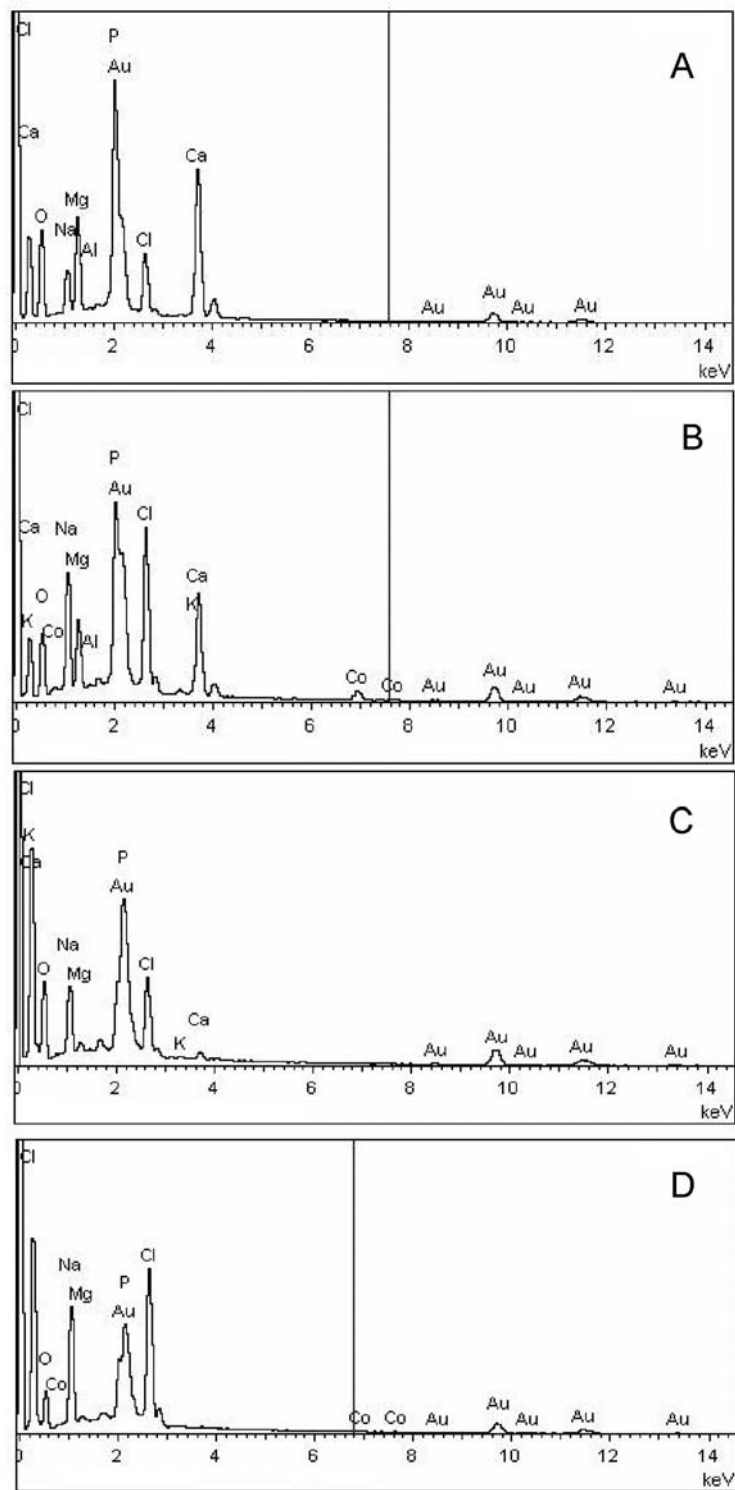


Fig 7

